that the noise cannot be related to the fluctuations of the CQW potential profile in the growth direction.

The appearance of the huge noise is strong evidence for the presence of coherence in the exciton system. Noise amplitude is known to be inversely proportional to the number of statistically independent entities in a system. Large noise amplitudes therefore denote that only a small number of entities exist in macroscopically large photoexcited region. The appearance of these macroscopic entities in the exciton system is consistent with the exciton condensation model. A condensed domain can be considered as one macroscopic entity. Due to the high oscillator strength of the exciton condensate, the PL signal of condensed excitons is much higher than for uncondensed ones. The formation and disappearance of condensed domains therefore results in fluctuations of the total PL signal. The noise appears in the range of B where τ_r^{-1} starts to increase and disappears in the range of B where τ_r^{-1} saturates and rapid exciton transport is observed. In the frame of the exciton condensation model the noise can be understood as the fluctuations near the phase transition connected with the instability of the condensed domains.

In conclusion, the observed set of anomalies in the transport and PL of indirect excitons in AlAs/GaAs CQWs is evidence for exciton condensation at low temperatures and high magnetic fields. The role of the magnetic field is the improvement of the critical conditions for the exciton condensation. The range of the magnetic fields studied can be divided into three parts. At low magnetic fields both the exciton transport and oscillator strength are characteristic for normal non-condensed excitons in a random potential: the diffusion coefficient increases with temperature, the oscillator strength only weakly depends on the temperature. At the highest studied magnetic fields both the exciton diffusion coefficient and the oscillator strength are anomalously large and decrease with temperature; this is consistent with the expected onset of exciton superfluidity and superradiance of exciton condensate. At intermediate magnetic fields a huge noise in the integrated PL intensity is observed under cw photoexcitation; the noise is consistent with fluctuations near the phase transition.

This work was performed in collaboration with A Zrenner, A I Filin, M Hagn, G Abstreiter, G Böhm, and G Weimann. We thank G E W Bauer, A B Dzyubenko, A Imamoglu, Yu M Kagan, V D Kulakovskiĭ, Yu E Lozovik, and B V Svistunov for interesting discussions. The work was supported financially by the Russian Foundation for Fundamental Research, the Russian Foundation for Nanostructures, and the Volkswagen Foundation.

References

1. Keldysh L V, Kopaev Yu E *Fiz. Tverd. Tela* (Leningrad) **6** 6219 (1965)
2. Hulin D, Mysyrowicz A, Benoit a la Guillaume C *Phys. Rev. Lett.* **45** 1970 (1980)
3. Timofeev V B, Kulakovskii V D, Kukushkin I V *Physica B* **117 – 118** 327 (1983)
4. Lin J L, Wolfe J P *Phys. Rev. Lett.* **71** 1222 (1993)
5. Kuramoto Y, Horie C *Solid State Commun.* **25** 713 (1978)
6. Lerner I V, Lozovik Yu E *Zh. Eksp. Teor. Fiz.* **80** 1488 (1981) [*Sov. Phys. JETP* **53** 763 (1981)]
7. Kagan Yu M, unpublished; for the infinite 2D systems the critical temperature for a phase transition to a superfluid state at $B = 0$ also roughly linearly depends on the density, see e.g. Fisher D S, Hohenberg P C *Phys. Rev. B* **37** 4936 (1988)
8. Butov L V et al. *Phys. Rev. B* **46** 12765 (1992)
9. Lozovik Yu E, Yudson V I *Zh. Eksp. Teor. Fiz.* **71** 738 (1976) [*Sov. Phys. JETP* **44** 389 (1976)]
10. Shevchenko S I *Fiz. Nizk. Temp.* **2** 251 (1976) [*Sov. J. Low Temp. Phys.* **2** 251 (1976)]
11. Zhu X et al. *Phys. Rev. Lett.* **74** 1633 (1995)
12. Bauer G E W, in *Optics of Excitons in Confined Systems* (Institute of Physics Conference Series No. 123, Eds A D'Andrea et al.) (Bristol, Eng.; Philadelphia: Institute of Physics, 1992) p. 283
13. Rashba E I, Gurgenishvilli G E *Fiz. Tverd. Tela* (Leningrad) **4** 1029 (1962) [*Sov. Phys. Solid State*]
14. Kash J A et al. *Phys. Rev. Lett.* **66** 2247 (1991)
15. Yoshioka D, MacDonald A H *J. Phys. Soc. Jpn.* **59** 4211 (1990)
16. Gilliland G D et al. *Phys. Rev. Lett.* **71** 3717 (1993)
17. Dzyubenko A B, Bauer G E W *Phys. Rev. B* **51** 14524 (1995)
18. Butov L V et al. *Phys. Rev. Lett.* **73** 304 (1994)

A self-assembled InAs quantum dot used as a quantum microscope looking into a two-dimensional electron gas

T Ihn, A Thornton, I E Itskevich, P H Beton, P Martin, P Moriarty, E Müller, A Nogaret, P C Main, L Eaves, M Henini

In the last decades our knowledge about two-dimensional electron gases (2DEGs) at low temperatures and in magnetic fields has tremendously grown and theoretical concepts have been developed describing their properties on a quantum mechanical basis and on a nanometer scale. Experiments are now desirable which test the predictions of these concepts not only on a macroscopic scale but using local probes of nm-size. We are able to probe the emitter 2DEG of a single-barrier tunneling device locally with a single InAs quantum dot [1 – 3]. The method has significant advantages over 2D – 2D tunneling experiments [4]. The dot is a local probe typically of 10 nm diameter and the tunneling characteristics are not smeared out by impurities. The discrete character of the dot state allows us to do energy spectroscopy by tuning the bias voltage. In contrast to conventional parallel magnetotransport measurements not only Fermi-level properties of the 2DEG can be observed but states (e.g. Landau levels) below the Fermi energy can be probed in a magnetic field [2, 3]. In addition, the properties of a single dot are of their own interest. Our measurements give us the opportunity to observe spin-splitting of the ground state of a single quantum dot.

The samples are single barrier n – i – n tunneling devices grown by MBE at 520 °C on the (100) surface of a GaAs n^+-substrate. Using the Stranski – Krastanov growth mode, self-assembled InAs quantum dots have been incorporated on the centre plane of the 10 nm AlAs barrier. The barrier is sandwiched between 100 nm undoped GaAs buffers on both sides. Graded n-type doping allows Ohmic contacts to be made on the top and the substrate side. Mesa structures typically of 50 μm diameter were fabricated by standard photolithography.

A typical dot size of 10 nm and a dot density of 10^{11} cm^{-2} was deduced from Scanning Tunneling Microscopy (STM) and Scanning Electron Microscopy (SEM) on similarly grown wafers. From cross-sectional transmission electron microscopy (XTEM) we get a direct insight into the wafer grown for the transport measurements. The height of the dots

is found to be 2–3 nm. Due to the finite dot height the tunneling barrier below the quantum dots appears to be slightly thicker than that on top. Nevertheless, both GaAs/AlAs heterointerfaces are of good quality and the quantum dots show a perfect crystal structure. Slight lattice distortions in and around the dots can be seen in XTEM pictures. They are due to a lattice mismatch of approximately 7% between InAs and AlAs.

Capacitance-voltage measurements at frequencies between 30 Hz and 1 MHz can be interpreted with a plate capacitor model. At zero bias the measured capacitance is determined by the distance between the doped top and bottom contact. Up to biases of 100 mV the capacitance increases strongly due to the formation of a 2DEG on the emitter side of the barrier (see inset of Fig. 1). This process effectively decreases the separation between capacitor plates and therefore increases the capacitance. From magneto-capacitance measurements we obtain the electron concentration and the (density dependent) elastic scattering time in the 2DEG. Magneto-oscillations can be observed at biases as low as 90 mV corresponding to an electron density of 3.5×10^{10} cm^{-2}.

Due to the placement of the dot layer in this plate capacitor the energy levels of the zero-dimensional (0D) dot states are shifted relative to the chemical potentials of the contacts (plates) when a voltage is applied (inset of Fig. 1). The leverage factor $f = \left[\partial E_{\mathrm{dot}}/\partial(eV)\right]^{-1}$ (~ 10 in our devices) allows the direct conversion of measured voltage differences into energy shifts.

We measure current–voltage $I(V)$ characteristics with a standard DC-setup and achieve a current-noise ratio of less than 50 fA. The measurements were performed in the temperature range from 4.2 K down to 70 mK applying magnetic fields up to 13 T.

The gross behavior of $I(V)$ traces is the same with current flow from or to the substrate as one would expect for a symmetric device. However, some structure which depends on the polarity of the applied voltage occurs on top of the sub-pA background current at low bias. In the following, the current flow from the substrate to the top contact is referred to as the forward bias direction.

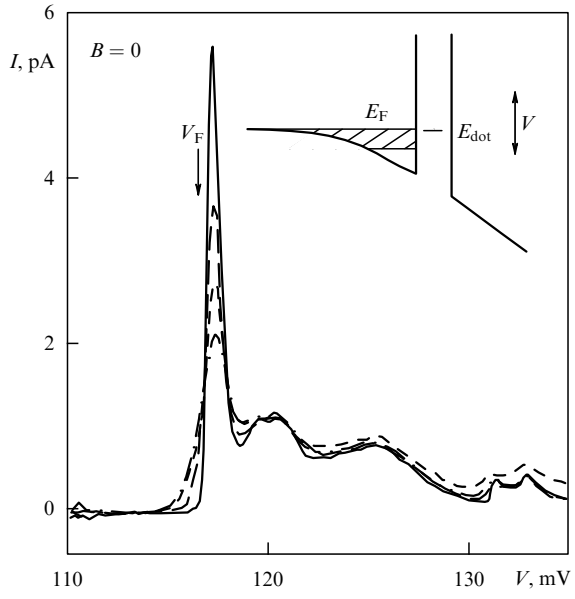

Figure 1. Temperature dependence of a single isolated resonance. The inset schematically shows the conduction band profile near the tunneling barrier.

At zero magnetic field and a forward bias below 300 mV isolated peaked structures with typical peak currents of 1–2 pA are observed in the $I(V)$ characteristics of most devices. An example is shown in Fig. 1. The structure is due to 2D–0D single-electron tunneling through an individual InAs quantum dot [2]. In reverse bias, steps occur in the tunneling current instead of peaks. This asymmetry of forward and reverse bias can be understood considering the above mentioned different barrier thicknesses above and below the dot layer. In both cases the onset of the current occurs when the energy level of an individual dot becomes resonant with the chemical potential of the emitter. In forward bias, the tunneling rate into the dot, given by $1/\tau_{\mathrm{in}} = I/e \approx 1/100$ ns, is much smaller than the tunneling-out rate of $1/\tau_{\mathrm{out}} \geqslant 1/50$ ps (its estimation will be explained later). Therefore the total tunneling current can be described as a sum of elastic and inelastic tunneling-in contributions, $I = I_{\mathrm{e}} + I_{\mathrm{i}}$. When the voltage is large enough to pull the dot energy below the subband bottom of the emitter 2DEG only I_{i} typically of 0.2 pA survives leading to a cut-off in the observed current. This allows us to estimate the inelastic tunneling rate to be $1/\tau_{\mathrm{i}} \sim 1/800$ ns and the elastic rate $1/\tau_{\mathrm{e}} \sim 1/110$ ns. In reverse bias, however, a constant tunneling current beyond the onset can only be observed if the ratio of the inelastic tunneling-in rate to tunneling-out rate is large compared to the relative accuracy of the current measurement of approximately 5%. In reverse bias we therefore estimate $1/\tau_{\mathrm{i}} \geqslant 1/5$ ns.

The isolated peaks occuring at low forward bias allow us (1) to probe local properties of the emitter 2DEG at the position of the quantum dot; (2) to explore properties of the quantum dot. In addition, interaction effects between the 2DEG and the tunneling electron are observed.

In forward bias the spectral sharpness of the dot state is determined by the tunneling-out rate. The current onset of an isolated resonance is found to be thermally activated according to $I \propto \exp\left[-(E_{\mathrm{dot}} - E_{\mathrm{F}})/kT\right]$ above 150 mK. This implies that down to this temperature the dot state is sharp enough to map out the Boltzmann-tail of the Fermi-distribution function in the emitter 2DEG. This confirms an energy resolution for the measurement better than 12 μeV, corresponding to a tunneling-out rate of $1/\tau_{\mathrm{out}} \geqslant 50$ ps in forward bias.

Typically, at the lowest temperatures a current enhancement is observed just beyond the current onset at V_{F}, as shown in Fig. 1. Increasing the temperature causes a significant decrease of the area under this Fermi-edge singularity (FES) peak, consistent with a many-body effect. It results from the interaction of the tunneling electron with the emitter 2DEG which opens additional tunneling channels. Although this effect is well known in tunneling experiments [5] it had not been possible before to study its behavior systematically at finite magnetic fields normal to the plane of the 2DEG. In our samples the evolution of the FES at finite magnetic field, B, can be unambiguously followed since the current enhancement is so pronounced relative to the single-particle current of typically 1 pA. We characterize the strength of the FES using the peak current $I_{\mathrm{peak}}(B)$ defined as the maximum current of the FES singularity feature at the lowest temperature. For some fields $I_{\mathrm{peak}}(B)$ falls below the typical single-electron current of 1 pA which we interpret as

the absence of the FES. It is noteworthy that the FES persists even in the region of $\nu < 1$. We have observed FES enhancements for B as high as 11 T.

In order to relate the applied magnetic field to a filling factor characterizing the state of the 2DEG we employ the onset voltage $V_F(B)$, experimentally defined as the voltage where the current exceeds a predefined limit of 1 pA (a slightly different value does not affect the results). In our devices the Fermi energy of the 2DEG, E_F, is pinned by the Fermi energy of the heavily doped contact which is itself given by the applied voltage V. At fixed V, changes in the density of states of the 2DEG caused by the magnetic field result in a self-consistent rearrangement of the 2DEG density n_S and $E_F - E_{dot}$ which are uniquely related [6]. Therefore $V_F(B)$, at which $E_F - E_{dot} = 0$, is a unique measure of n_S and the filling factor ν.

Figure 2 shows a typical example of $V_F(B)$ and $I_{peak}(B)$. The onset voltage $V_F(B)$ oscillates periodically in $1/B$ and I_{peak} exhibits minima for fields $B = 1.85$, 0.92 and 0.46 T which correspond to filling factors $\nu = 1, 2, 4$, respectively. Theories for $B = 0$ predict the strength of the FES to be proportional to the density of states at the Fermi-energy of the 2DEG [7, 8]. Our experimental results suggest that this prediction is also valid for finite magnetic fields up to filling factor $\nu = 1$. Details of the FES behavior at fractional filling factors will be published elsewhere.

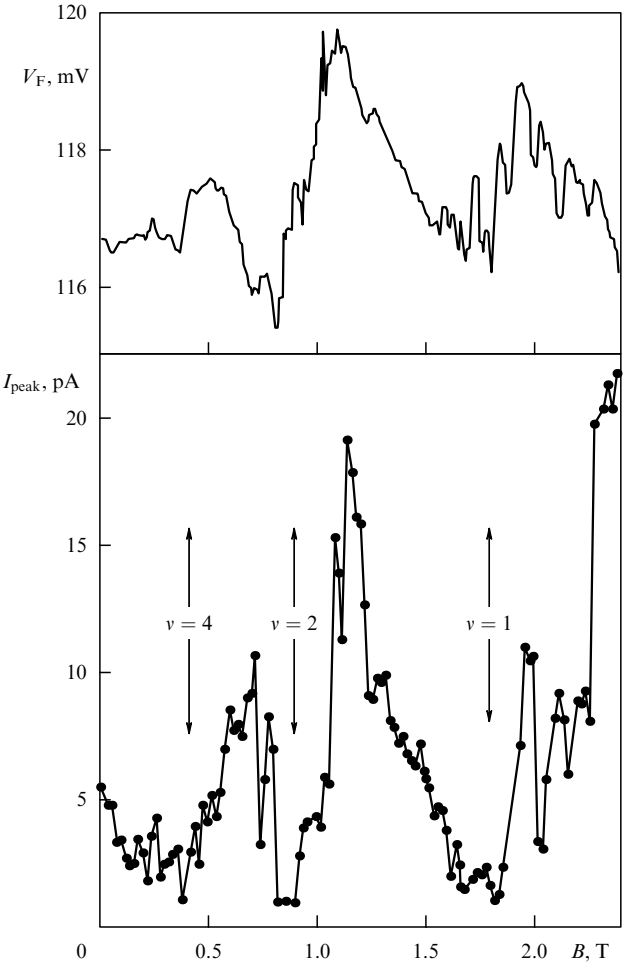

Figure 2. Oscillation of the onset voltage V_F and the peak current I_{peak} with B in the regime of integer filling factors ν.

The fine structure visible in $V_F(B)$ around the integer filling factors is reproducible in detail and reflects mesoscopic properties of the two-dimensional electron gas [3]. This and related effects are most pronounced when the density of states at the Fermi-energy is low and screening is weak.

Although sharp photoluminescence lines due to single InAs dots have been reported [9] no observations of spin splitting in a magnetic field were made. The g-factor of InAs dots at high magnetic fields can be obtained from capacitance spectroscopy [10], but there is some uncertainty in the results. In our system the spin-splitting of a single InAs quantum dot state can be observed with a magnetic field applied parallel to the emitter 2DEG [11]. Figure 3 shows the evolution of a single-dot resonance feature with increasing magnetic field. At $B = 4$ T the current onset has split into two separate onsets, at $B = 8$ T two separate peaks are visible. The onset splitting is linear in magnetic field. The difference in the onset voltages of the two peaks marks the onset of resonant tunneling through two different spin-channels in the quantum dot. The Zeeman splitting of the dot state $\Delta E = g\mu_B B$ is related to the voltage splitting via the leverage factor f. A Lande-factor $g = 0.82 \pm 0.09$ has been determined from the data in strong contrast to the InAs bulk value of $g = -15$. This strong discrepancy with the bulk value can be understood in terms of a $(\mathbf{k}, \mathbf{p})$-model. The strong confinement of the state in the dot and the strain will give the main contributions to the g-factor change.

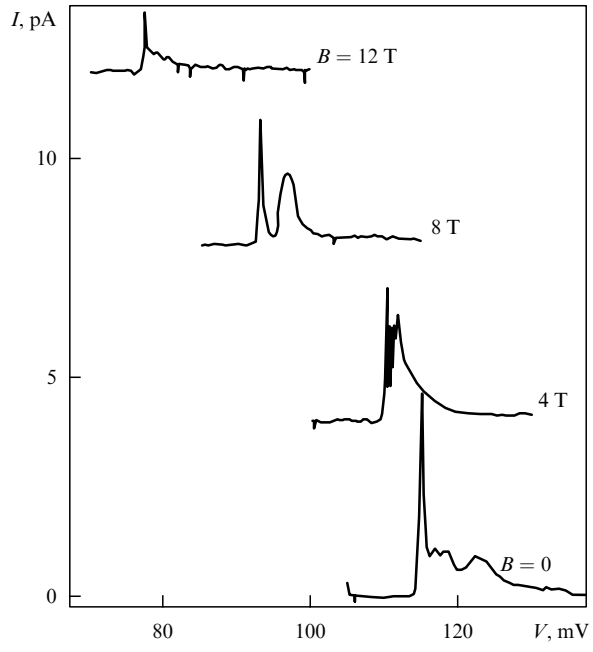

Figure 3. Spin splitting of a single dot state as observed in the tunneling current.

In conclusion, we are able to probe the properties of a 2DEG in a magnetic field on a local scale using a single self-assembled InAs quantum dot. Interaction effects between the 2DEG and the tunneling electron turn out to give important many-body contributions to the tunneling current. The spin-splitting of the ground state of a single quantum dot in a magnetic field is observed and a g-factor of $g = 0.82 \pm 0.09$ can be deduced.

This work was supported by EPSRC (UK), the Russian Foundation for Fundamental Research (Grant 97-02-17802) and GNTP "Nanostructures" (Grant 97-1068). I.E.I. and L.E. acknowledge the support from The Royal Society and from EPSRC for a Senior Fellowship, respectively.

References

1. Itskevich I E et al. *Jpn. J. Appl. Phys.* **36** 4073 (1997)
2. Itskevich I E et al. *Phys. Rev. B* **54** 16401 (1996); Thornton A et al. *Superlattices and Microstructures* **21** 255 (1997)
3. Thornton A et al., in *Proc. of the Int. Conf. on High Magnetic Fields in Semiconductor Physics, Würzburg, Germany* (1996) p. 473
4. Eisenstein J P, Pfeiffer L N, West K W *Phys. Rev. Lett.* **69** 3804 (1992); *Phys. Rev. Lett.* **74** 1419 (1995) (and references therein)
5. Geim A K et al. *Phys. Rev. Lett.* **72** 2061 (1994)
6. Böckenhoff E, von Klitzing K, Ploog K *Phys. Rev. B* **38** 10120 (1988); Chan K S et al. *Phys. Rev. B* **56** 1447 (1997)
7. Mahan G D *Many-Particle Physics* 2nd edition (New York: Plenum, 1990) p. 732
8. Matveev K A, Larkin A I *Phys. Rev. B* **46** 15337 (1992)
9. Fafard S et al. *Phys. Rev. B* **50** 8086 (1994); Grundmann M et al. *Phys. Rev. Lett.* **74** 4043 (1995)
10. Fricke M et al., in *Proc. 23d Int. Conf. on the Physics of Semiconductors, Berlin* (Eds M Scheffler, R Zimmermann) (Singapore: World Scientific, 1996) p. 1609
11. Thornton A S G et al. *Int. Conf. MSS 1997, Santa Barbara, USA*